PLOS ONE

RESEARCH ARTICLE

Incorporating the thermodynamic effects of temperature and pressure on modeling neuronal gating kinetics

Jake A. Miller[1], **Bahram Pahlavan**[1], **Bryan Gamboa**[2], **Fidel Santamaria**[1]*

1 Department of Neuroscience, Developmental and Regenerative Biology, College of Sciences, The University of Texas at San Antonio, San Antonio, Texas, United States of America, **2** Air Force Research Laboratory the Human Performance Wing, Human Effectiveness Directorate, Bioeffects Division, Radio Frequency Bioeffects Branch, Joint Base San Antonio Fort Sam Houston, Texas, United States of America

* fidel.santamaria@utsa.edu

OPEN ACCESS

Citation: Miller JA, Pahlavan B, Gamboa B, Santamaria F (2025) Incorporating the thermodynamic effects of temperature and pressure on modeling neuronal gating kinetics. PLoS One 20(10): e0333592. https://doi.org/10.1371/journal.pone.0333592

Editor: Ghanim Ullah, University of South Florida, UNITED STATES OF AMERICA

Received: March 11, 2025

Accepted: September 16, 2025

Published: October 9, 2025

Data availability statement: All simulation files, analysis scripts, and data are available in https://github.com/SantamariaLab or by request. They are also in ModelDB (https://modeldb.science/2019887) data base Model Number 2019887.

Funding: BG AFOSR LRIR 23RHCOR012 FS NIH-NINDS 1R01NS130759. AFOSR LRIR: Air Force office of Scientific Research - Laboratory Research Initiation Request. NIH-NINDS: National Institutes of Health-National Institute of

Abstract

Temperature and pressure affect neuronal gating kinetics. We recently used thermodynamic macro-molecular rate theory to describe the effects of temperature on the activation rate function of sodium, potassium, and calcium voltage activated conductances. Here, we extend the theory to include the effects of both, temperature and pressure. The theory includes transition changes in heat capacity, entropy, enthalpy, activation volume, expansivity, and compressibility during protein conformation. The complete model replicates experimental results from the literature. We used the expanded model to study how temperature and pressure affect the generation of action potentials in the Hodgkin-Huxley model and in detailed biophysical and morphological models of human cortical neurons. In particular, our results show how pressure can affect the optimal temperature of reaction rates and how small changes in pressure could affect spike timing and correlations across neurons. Our work provides a physics-based approach to adjust reaction rates of neuronal conductances to study cellular function in evolution and under extreme heat and pressure conditions such as those found in blast waves or electro-mechanical neuronal couplings.

Introduction

Practically all studies on the effects of temperature [1–6] and pressure [7–9] on the activation rate of voltage-gated conductances use an exponential function: either Q_{10}, the Arrhenius function [10], or its related transition state theory [11]. This approach assumes that temperature only affects the free energy ($\Delta G^{\ddagger}$) of the energy barrier of the activation gating mechanism through constant entropy ($\Delta S^{\ddagger}$) and enthalpy ($\Delta H^{\ddagger}$). However, macroproteins show a universal non-Arrhenius temperature-dependent behavior characterized by a decrease in reaction rate after an optimal temperature (T_{opt}) not due to denaturation [12]. We recently used Macromolecular Rate Theory (MMRT) to demonstrate that sodium (Na), potassium (K), and calcium (Ca) membrane conductances all have T_{opt} within physiological ranges not

Neurological Disorders. The funders had no role in study design, data collection and analysis, or preparation of the manuscript. The views expressed are those of the author and do not reflect the official guidance or position of the United States (U.S.) Government, Department of Defense, United States Air Force or United States Space Force. Distribution A: Approved for public release; distribution unlimited (P.A. #AFRL-2024-0248, 16 JAN 2024).

Competing interests: The authors have declared that no competing interests exist.

associated with denaturation and that the Arrhenius equation produces additive errors in predicting temperature effects [13]. The MMRT assumes that temperature affects both the enthalpy and entropy of the energy barrier through changes in the heat capacity ($\Delta C_p^{\ddagger}$) of enzymes.

There is a great deal of interest in understanding how thermodynamic variables affect enzymatic function [14,15]. For example, temperature [16,17], pressure [18–22], and osmotic flow [23,24]. In particular, there are multiple studies to understand how temperature [1,25–28] and pressure [29–32] affect neuronal function. A unified model could be useful for a wide range of applications, such as the effects on cellular function in extremophilic bacteria [33] and deep-sea marine organisms [20,21,34]. This would also be of interest in understanding neuronal function. For example, the heat and pressure waves of a concussive blast [35,36] or electro-mechanical neuronal couplings affecting anesthesia [37,38].

In this study, we extend our MMRT-based approach [13] to integrate the effects of pressure [39], providing a quantitative thermodynamic description of voltage-gated membrane conductances behavior. We first develop the theory and then we evaluate the validity of its parameters through data fitting. We then use the model to understand how the effects of temperature and pressure on voltage gated conductances impact action potential generation, firing frequency, and precise timing. We conclude by exploring physical interpretations of the parameters in the model.

Theory

Macromolecular rate theory. The value of $\Delta G^{\ddagger}$ between the ground and transition state of an ion channel is:

$$\Delta G^{\ddagger} = \Delta H^{\ddagger} - T\Delta S^{\ddagger} \tag{1}$$

Changes in heat, $\Delta Q^{\ddagger}$, are related to $\Delta H^{\ddagger}$ and $\Delta S^{\ddagger}$ via $\Delta C_p^{\ddagger}$ when $\Delta P^{\ddagger} = 0$:

$$d\Delta Q = \Delta C_p^{\ddagger} dT = Td\Delta S^{\ddagger} = d\Delta H^{\ddagger} \tag{2}$$

Integrating assuming constant $\Delta C_p^{\ddagger}$ [17], to get $\Delta S^{\ddagger}$ and $\Delta H^{\ddagger}$ and substitute in Eq 1, we get the basis of MMRT.

$$\begin{aligned}\Delta G_{MMRT}^{\ddagger} = \Delta C_p^{\ddagger}(T - T_o) - \Delta C_p^{\ddagger} T \ln(T/T_o) \\ - T\Delta S_o^{\ddagger} + \Delta H_o^{\ddagger}\end{aligned} \tag{3}$$

where $\Delta S_o^{\ddagger}$, and $\Delta H_o^{\ddagger}$ correspond to a reference temperature T_o.

The rate coefficient function is based on the Eyring equation, Eq 4.

$$k = \frac{k_B T}{h} e^{-\Delta G^{\ddagger}/RT} \tag{4}$$

where k_B and h, are Boltzmann's and Planck's constants, respectively, and R is the universal gas constant. The value of T_{opt} is where $\frac{dk}{dT} = 0$ [13,16,40].

Incorporating the effects of pressure. The effect of pressure, P, on a reaction rate is mediated by the activation volume, $\Delta V^{\ddagger}$ [41,41–44]:

$$k_P = k_o e^{-(P-P_o)\Delta V^{\ddagger}/RT} \tag{5}$$

Several studies suggest a positive change in $\Delta V^{\ddagger}$ for ion channel opening conformations [29–32,45–48]. Based on [39] and [19,21,22]:

$$dG = -SdT + VdP \tag{6}$$

Entropy depends on temperature and pressure

$$dS = \left.\frac{\partial S}{\partial T}\right|_P dT + \left.\frac{\partial S}{\partial P}\right|_T dP \tag{7}$$

Using Eq 2 for $\Delta C_p^{\ddagger}$ and the Maxwell relation $\left.\frac{\partial S}{\partial P}\right|_T = -\left.\frac{\partial V}{\partial T}\right|_P$ we get:

$$dS = \frac{C_p}{T}dT - \left.\frac{\partial V}{\partial T}\right|_P dP \tag{8}$$

The isobaric thermal volume is $\hat{\alpha} = \alpha V$ with α the expansivity coefficient:

$$\alpha = \frac{1}{V}\left.\frac{\partial V}{\partial T}\right|_P \tag{9}$$

Thus,

$$dS = \frac{C_p}{T}dT - \hat{\alpha}dP \tag{10}$$

Similarly for volume:

$$dV = \left.\frac{\partial V}{\partial T}\right|_P dT + \left.\frac{\partial V}{\partial P}\right|_T dP \tag{11}$$

Using the isothermal volume compressibility, $\hat{\kappa} = \kappa V$, with the compressiblity coefficient, $\kappa = -\frac{1}{V}\left.\frac{\partial V}{\partial P}\right|_T$, we get

$$dV = \hat{\alpha}dT - \hat{\kappa}dP \tag{12}$$

Assuming that C_p, $\hat{\alpha}$, and $\hat{\kappa}$ are temperature and pressure independent, the integrals are:

$$S - S_o = C_p \ln|T/T_o| - \hat{\alpha}(P - P_o) \tag{13a}$$

$$V - V_o = \hat{\alpha}(T - T_o) - \hat{\kappa}(P - P_o) \tag{13b}$$

Where T_o, is a reference temperature with associated reference values P_o, S_o and V_o. We substitute in Eq 6.

$$\begin{aligned} G(T,P) = {} & C_p(T - T_o - T\ln|T/T_o|) - S_o(T - T_o) \\ & + \hat{\alpha}(T - T_o)(P - P_o) + V_o(P - P_o) \\ & - \frac{\hat{\kappa}}{2}(P - P_o)^2 + G_o \end{aligned} \tag{14}$$

We can convert this into values for the change between the ground and the transition state of the reaction. Because MMRT uses $\Delta H_o^{\ddagger}$, we can make the substitution $G_o = H_o - T_oS_o$ and

ultimately produce:

$$\begin{aligned}\Delta G^{\ddagger} =& \Delta C_p^{\ddagger}\left[(T - T_o) - T\ln\left|T/T_o\right|\right] - T\Delta S_o^{\ddagger} \\ &+ \Delta\hat{\alpha}^{\ddagger}(T - T_o)(P - P_o) + \Delta V_o^{\ddagger}(P - P_o) \\ &- \frac{\Delta\hat{\kappa}^{\ddagger}}{2}(P - P_o)^2 + \Delta H_o^{\ddagger}\end{aligned} \tag{15}$$

Where $\Delta\hat{\alpha}^{\ddagger} = \Delta(\alpha V)^{\ddagger}$ and $\Delta\hat{\kappa}^{\ddagger} = \Delta(\kappa V)^{\ddagger}$. Eq 15 incorporates the terms from Eq 3 and Eq 5. To obtain the kinetics, we plug Eq 15 into Eq 4.

The activation volume as a function of pressure and temperature is found in Eq 13b as:

$$\Delta V^{\ddagger} = \Delta\hat{\alpha}^{\ddagger}(T - T_o) - \Delta\hat{\kappa}^{\ddagger}(P - P_o) + \Delta V_o^{\ddagger} \tag{16}$$

The value of T_{opt} is:

$$\begin{aligned}T_{opt} = &\left[\Delta C_p^{\ddagger}T_o - \Delta H_o^{\ddagger} + \Delta\hat{\alpha}^{\ddagger}T_o(P - P_o)\right. \\ &\left. - \Delta V_o^{\ddagger}(P - P_o) + \frac{\Delta\hat{\kappa}^{\ddagger}}{2}(P - P_o)^2\right]/(\Delta C_p^{\ddagger} + R)\end{aligned} \tag{17}$$

Materials and methods

We used our previous parametrization of MMRT for the values of $\Delta C_p^{\ddagger}$ and $\Delta H_o^{\ddagger}$ [13]. As we did before, the values of $\Delta S_o^{\ddagger}$ were adjusted so $k = 1$ at $T = 20°C$. The reference temperature and pressure were $T_o = 25°C$ and $P_o = 1$ atm, respectively.

We conducted a literature search for experimental data on the effects of pressure on the kinetics of voltage-gated channels[29–32,45,47–49]. We used the results from these papers to determine the other parameters, see Table 1.

Studies on the squid's giant axon [30–32] reported values of $\Delta V^{\ddagger}$, Table 1. We assumed a linear relation between reference activation volume and temperature, which resulted in $\Delta V_o^{\ddagger} = 19\text{cm}^3\text{mol}^{-1}$ at T_o. The values for $\Delta V_{Na}^{\ddagger}$ and $\Delta V_K^{\ddagger}$ were very close to each other [30,31], so we used their average for the simulations.

From the values of $\Delta V_{Na}^{\ddagger}$ and $\Delta V_K^{\ddagger}$ at different temperatures and using Eq 16 we calculated an average value of $\Delta\hat{\alpha}^{\ddagger} = -1\text{cm}^3\text{mol}^{-1}\text{K}^{-1}$, which is consistent with an earlier report [47]. The

Table 1. Parameter values for generating figures based on the thermodynamic model. The values for $\Delta C_p^{\ddagger}$, $\Delta S_o^{\ddagger}$, and $\Delta H_o^{\ddagger}$ were obtained from our previous publication [13].

	Na	K	Ca	Units
$\Delta C_p^{\ddagger}$	−2.76 ± 0.92	−1.70 ± 0.59	−5.07 ± 3.58	kJ mol^{-1}
$\Delta S_o^{\ddagger}$	−113 ± 38.90	−130 ± 7.77	−2.30 ± 138	J mol^{-1} K^{-1}
$\Delta H_o^{\ddagger}$	33.90 ± 1.40	31.80 ± 2.06	70.80 ± 1.11	kJ mol^{-1}
	5°C	10°C	15°C	Units
$\Delta V_{Na}^{\ddagger}$	44	35	30	cm^3 mol^{-1}
$\Delta V_K^{\ddagger}$	42	37	31	cm^3 mol^{-1}
		High	Low	Units
$\Delta\hat{\alpha}^{\ddagger}$		−1	10^{-2}	cm^3 mol^{-1} K^{-1}
$\Delta\hat{\kappa}^{\ddagger}$		10^4	10^2	cm^3 mol^{-1} GPa^{-1}
				Units
T_o		25		°C
P_o		1		atm
$\Delta V_o^{\ddagger}$		19		cm^3 mol^{-1}

https://doi.org/10.1371/journal.pone.0333592.t001

change in α across an increase in temperature was found to be negative [50,51] but positive for unfolding [51]. So, we might also estimate $\Delta\hat{\alpha}^{\ddagger}$ at a lower 10^{-2}cm^{3}mol^{-1}K^{-1}. Therefore, we estimate a high magnitude value of $\Delta\hat{\alpha}^{\ddagger} = -1$ and a low value of 10^{-2}.

From $\Delta\hat{\alpha}^{\ddagger} = \Delta(\alpha V)^{\ddagger}$ approximate $\Delta\hat{\alpha}^{\ddagger} \approx \alpha\Delta V^{\ddagger} + V\Delta\alpha^{\ddagger}$. Since the scale of $\Delta V^{\ddagger}$ is 10^2, and assuming both terms are approximately equal or the first dominates, the scale of $\alpha \approx 10^{-2}$K^{-1}. This is near reported values of α in the $10^{-4} - 10^{-3}$K^{-1} range [50–53] and will be fine for analyzing the impact of this parameter.

Dreydroppel et al. [39] provides a value for $\Delta\kappa^{\ddagger}$ of 1.8 GPa^{-1} with $\Delta\hat{\kappa}^{\ddagger}$ of 130cm^{3}mol^{-1}GPa^{-1}. Others reported compressibilities on the scale of 0.1GPa^{-1} [50,52,54]. Assuming the same $\Delta V^{\ddagger}$ as in [39] suggests a high value of $\Delta\hat{\kappa}^{\ddagger} = 10^4$.

Rapid changes in pressure could result in increases in temperature, known as adiabatic heating. Based on previous reports [31,46,47,49] we assume an adiabatic heating of 1°C per 20MPa (≈ 200atm).

We tested the thermodynamic effects of pressure and temperature on membrane conductance gating on neuronal models of action potential generation. First, we used a Hodgkin-Huxley system of equations. We multiplied the reaction rate of each conductance by the rate coefficient k normalized by modifying $\Delta S_o^{\ddagger}$ to the control experimental condition of 6.3°C, Eq 4. In another set of simulations, we chose four models from the Allen Brain Cell Types database. We used an identical approach as in our previous publication [13]. All simulation files, analysis scripts, and data are available in github.com/SantamariaLab or by request. They are also in ModelDB data base Model Number 2019887.

Results

Pressure effects on rate coefficient function

To gain intuition on how pressure affects the reaction rate coefficient of membrane conductances we plotted k (Eq 4 with Eq 15) as a function of temperature and pressure. We used our previously calculated averaged temperature thermodynamic parameters for Na conductances ($\Delta C_p^{\ddagger}$, $\Delta S_o^{\ddagger}$, $\Delta H_o^{\ddagger}$) and our estimated value of $\Delta V_o^{\ddagger} = 19$ cm^{3}mol^{-1}. For the expansivity and compressibility we used $\Delta\hat{\alpha}^{\ddagger} = -0.20$ cm^{3}mol^{-1}K^{-1}, and $\Delta\hat{\kappa}^{\ddagger} = 1\times10^2$ cm^{3}mol^{-1}GPa^{-1} because this combination resulted in decreasing values of the reaction rate as a function of pressure, consistent with experimental reports, see Table 1 and Methods. We plotted the value of k at three representative pressures (atmospheric pressure, 1atm; average ocean depth, ≈ 370atm; and bottom of the Mariana Trench, ≈ 1, 072atm), Fig 1A. With this combination of parameters the value of T_{opt} varied over a small range, from $T_{opt} = 38.25$ °C at 1 atm to $T_{opt} = 40.96$ °C at 1,000 atm, Fig 1B.

We wanted to calculate the value of $\Delta V_o^{\ddagger}$, based on electrophysiology recording and compare to our estimate. To do this we used the model to fit values of k extracted from experiments on different neurons and conductances [30–32,48,55], Fig 2. Depending on the source of experiments, we used the average temperature parameters we previously calculated for Na and K conductances. As we did in the past, we also fit the value of $\Delta S_o^{\ddagger}$ because this varies as a function of the experimental temperature and does not affect the rate of change of the MMRT function. In all fits we assumed $\Delta\hat{\alpha}^{\ddagger} = -0.20$ cm^{3}mol^{-1}K^{-1} and $\Delta\hat{\kappa}^{\ddagger} = 1\times10^2$ cm^{3}mol^{-1}K^{-1}. The fits had a mean R^2 of 0.93 ± 0.06. This analysis shows very accurate values of both parameters. The average value of $\Delta S_o^{\ddagger}$ was –133.97 ± 3.88 SD Jmol^{-1}K^{-1}, with an average 95% confidence interval of 1.16 ± 0.81 SD Jmol^{-1}K^{-1}. The values of $\Delta S_o^{\ddagger}$ were very close to those that we reported for potassium channels in our previous study. For $\Delta V_o^{\ddagger}$ the average value was 40.93 ± 11.60 SD cm^{3}mol^{-1} and a 95% confidence interval of 9.20 ± 6.47, which are in the range of values reported of Na and K conductances, see Table 1.

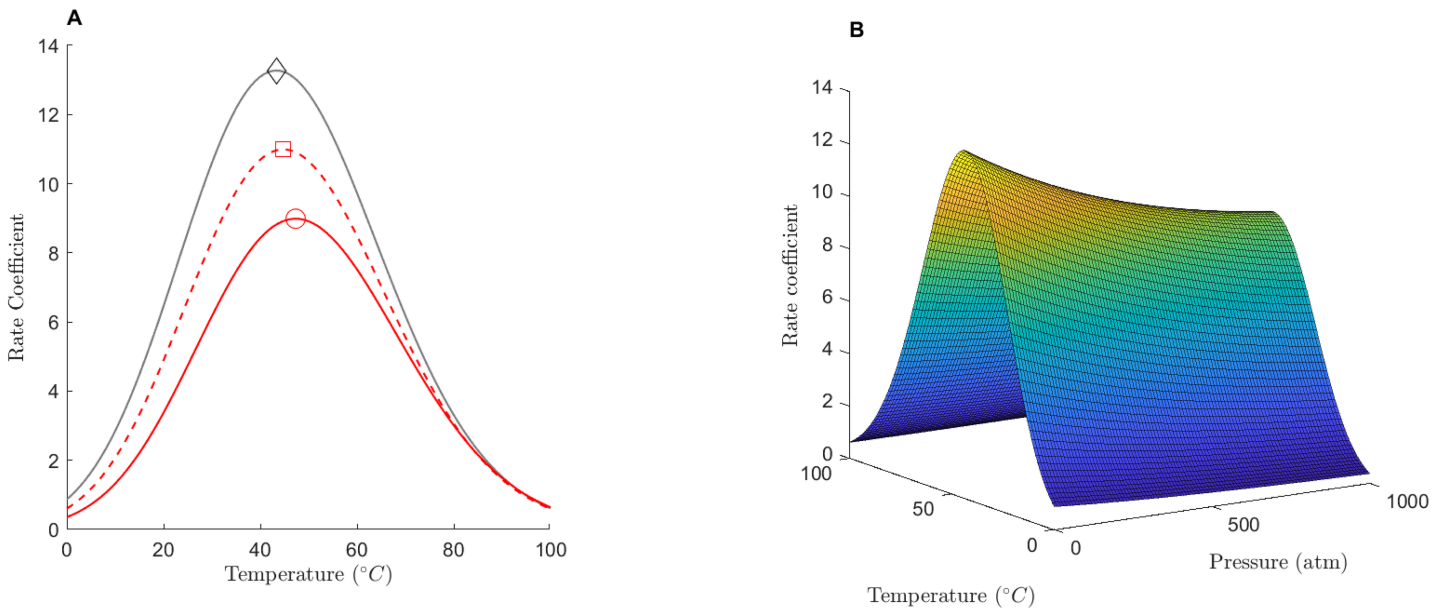

Fig 1. The effects of pressure on the reaction rate coefficient function of average sodium conductances. (**A**) Reaction rate coefficient vs temperature at 1 atm (⋄), average ocean depth ≈ 350 atm (□), and Mariana trench ≈ 1,072 atm (○). (**B**) The rate coefficient as a function of pressure and temperature. Parameters were: $\Delta C_p^{\ddagger} = -2.76 \times 10^3$ kJmol^{-1}, $\Delta S_o^{\ddagger} = -113$ Jmol^{-1}K^{-1}, $\Delta H_o^{\ddagger} = 34 \times 10^3$ kJmol^{-1}, and $\Delta V_o^{\ddagger} = 19$ cm^{3}mol^{-1}, $\Delta\hat{\alpha}^{\ddagger} = -0.20, 1 \times 10^{-2}$ and $\Delta\hat{\kappa}^{\ddagger} = 1 \times 10^2$ cm^{3}mol^{-1}GPa^{-1}.

https://doi.org/10.1371/journal.pone.0333592.g001

Adiabatic heating effects on pressure measurements

We studied the effects of incorporating adiabatic heating in the model, Fig 3. We plotted four isotherms of the rate coefficient function using $\Delta\hat{\alpha}^{\ddagger} = -0.2$ cm^{3}mol^{-1}K^{-1} and $\Delta\hat{\kappa}^{\ddagger} = 100$ cm^{3}mol^{-1}GPa. We applied a one-degree increase for every 20MPa (197atm) from rapid pressure change. Depending on the starting temperature, adiabatic heating temperature change can have a significant impact on the shape of k. The effect of rapid heating is minimal when the pressure change is at T_{opt}. At suboptimal temperatures, the heating increases rate whereas at supraoptimal temperatures heating is adverse. This behavior reflects the temperature optimum over rate and is a significant quantitative result that should be considered for rapid or transient pressure changes.

Sensitivity to expansivity, compressibility, and activation volume

In the previous sections we first calculated the value of $\Delta V_o^{\ddagger}$ to avoid over-parametrization and the numerical effects on the fitting procedure of parameters with large differences in their orders of magnitude and quadratic effects of temperature and pressure. Here we perform a sensitivity analysis of the model by varying the values of $\Delta\hat{\alpha}^{\ddagger}$ and $\Delta\hat{\kappa}^{\ddagger}$ and $\Delta V_o^{\ddagger}$, Fig 4.

We first studied how the model behaved when using the extreme values of $\Delta\hat{\alpha}^{\ddagger}$ and $\Delta\hat{\kappa}^{\ddagger}$, Fig 4A. We plotted the value of T_{opt}, k at T_{opt}, and at an experimental temperature, which we selected to be 21 °C, all as a function of pressure. When using the low value of $\Delta\hat{\kappa}^{\ddagger} = 10^2$ cm^{3}mol^{-1}GPa we obtained a linear relationship between T_{opt} with pressure independently of the value of $\Delta\hat{\alpha}^{\ddagger}$. When using $\Delta\hat{\alpha}^{\ddagger} = 10^{-2}$ cm^{3}mol^{-1}K^{-1} and $\Delta\hat{\kappa}^{\ddagger} = 10^2$ cm^{3}mol^{-1}GPa, which are found in soluble proteins [39,50–54], there is a minimum effect of pressure on T_{opt}. In contrast, when using the high value of $\Delta\hat{\kappa}^{\ddagger} = 10^4$ cm^{3}mol^{-1}GPa there is a non-linear behavior of T_{opt}. The analysis of the rate coefficient at T_{opt} or at 21 °C suggest that there are

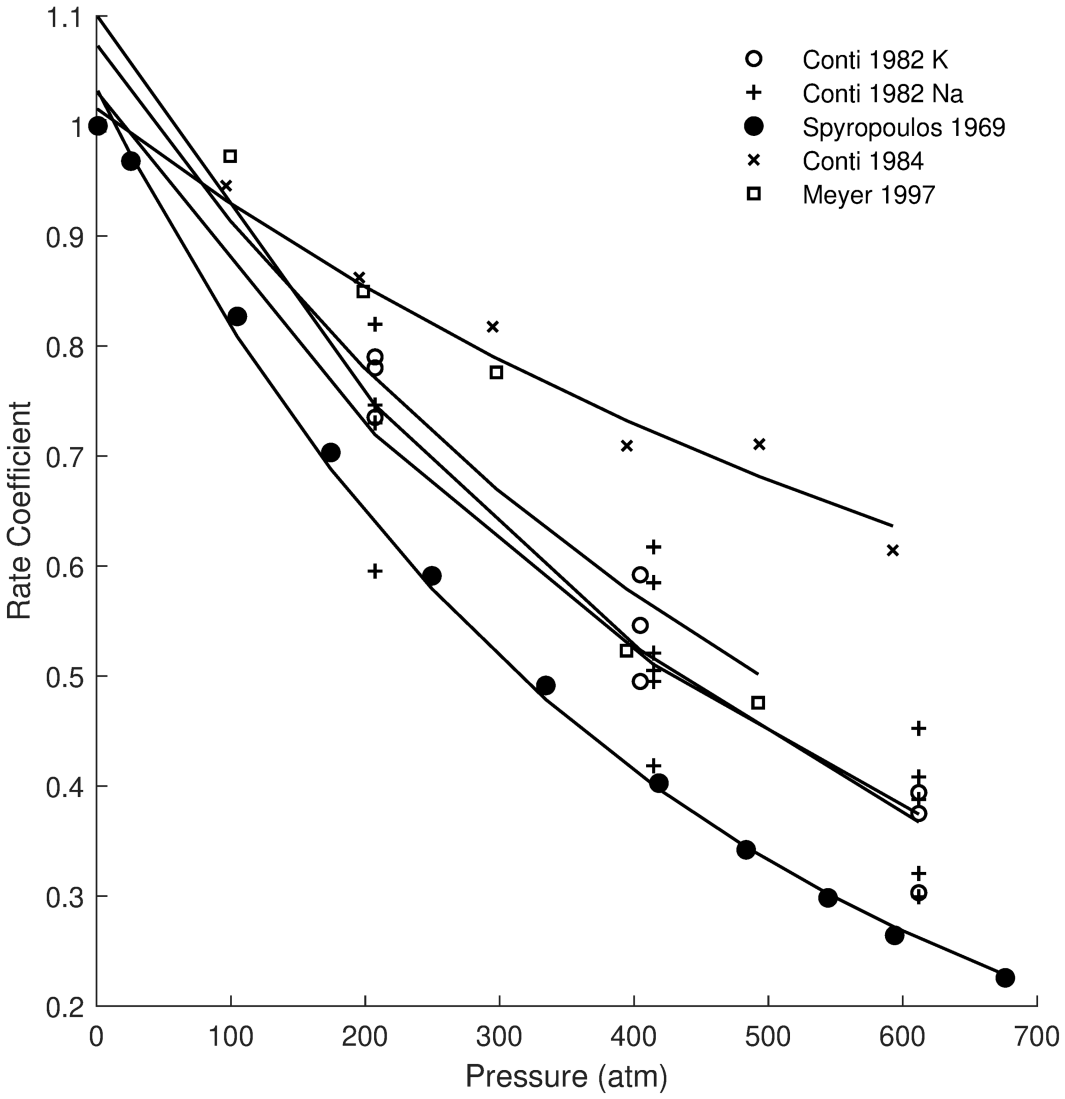

Fig 2. Fitting the model to experimental measurements of the rate coefficient as a function of pressure. Normalized experimental rate coefficient data [30–32,46,48,55] and model fits. See text for details.

https://doi.org/10.1371/journal.pone.0333592.g002

interactions between the values $\Delta\hat{\alpha}^{\ddagger}$ and $\Delta\hat{\kappa}^{\ddagger}$ that result in decreasing reaction coefficient behavior as a function of pressure.

To estimate the relative effect of varying the pressure parameters we took as a reference our model parametrized with $\Delta V_o^{\ddagger} = 40.96\text{cm}^3\text{mol}^{-1}$, $\Delta\hat{\alpha}^{\ddagger} = -0.20\text{cm}^3\text{mol}^{-1}\text{K}^{-1}$ and $\Delta\hat{\kappa}^{\ddagger} = 10^2\text{cm}^3\text{mol}^{-1}\text{GPa}^{-1}$, Fig 4B–4D. This shows that the behavior of T_{opt} is highly sensitive to the values of $\Delta\hat{\alpha}^{\ddagger}$. The behavior of the rate coefficient is sensitive at T_{opt} but is less at our designated experimental temperature. In contrast, the behavior of T_{opt} is not sensitive to the values of $\Delta\hat{\kappa}^{\ddagger}$ but could have a strong effect at experimental temperatures on the value of the rate coefficient. A similar effect is seen with the values of $\Delta V_o^{\ddagger}$. Taken together, this analysis provides a methodology to distinguish between the effects of each of these parameters on how the reaction coefficient function is affected by pressure.

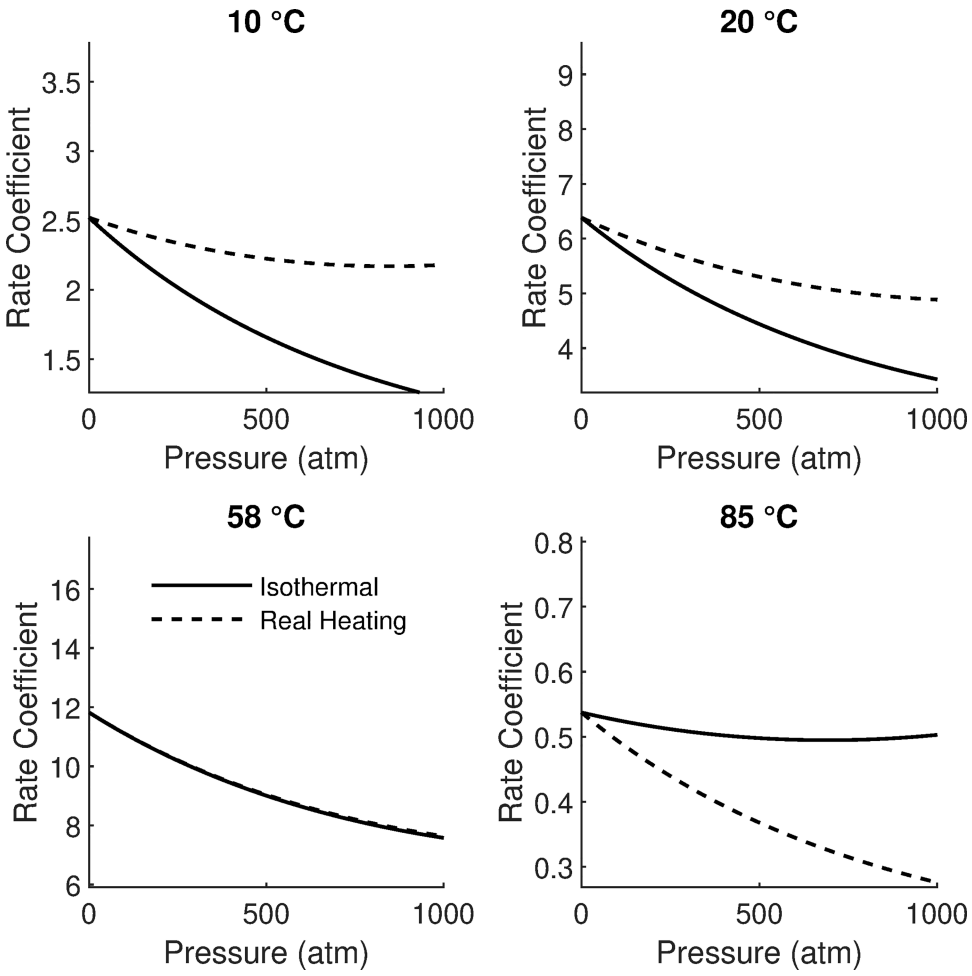

Fig 3. Pressure and adiabatic heating effects. The pressure dependence of rate is shown at multiple temperatures. Because increasing pressure can cause a temperature increase, we show that effect with the dashed line. The optimal temperature with the parameters used was 58°C and the rates are referenced at 20°C.

https://doi.org/10.1371/journal.pone.0333592.g003

Effects of temperature and pressure on action potential generation and timing

We performed an analysis of the spiking and firing rate of the Hodgkin-Huxley equations under different temperature and pressure conditions, Fig 5. Increasing pressure resulted in a broadening of the action potential and a lengthening of the inter-spike interval. However, at higher temperatures, pressure had a stabilizing effect on the shape of the action potential. In all cases, we used the $\Delta\hat{\alpha}^{\ddagger} = -0.2$ and $\Delta\hat{\kappa}^{\ddagger} = 100$, Fig 5A. The summary data, Fig 5B, shows a continuous decrease in firing rate due to pressure (top), a temperature dependence that peaks at 16°C, followed by a failure to generate action potentials past 21 °C, note that we required a minimum amplitude of 20 mV to detect an action potential) (center). We also see a similar behavior of firing rate as a function of input current (bottom).

The plots in Fig 5 suggest a weak pressure effect on action potential generation and average firing rate. However, in those plots, we noticed an effect on spike timing. To study the possibility that pressure could affect spike timing, but not firing rate, we performed a series of

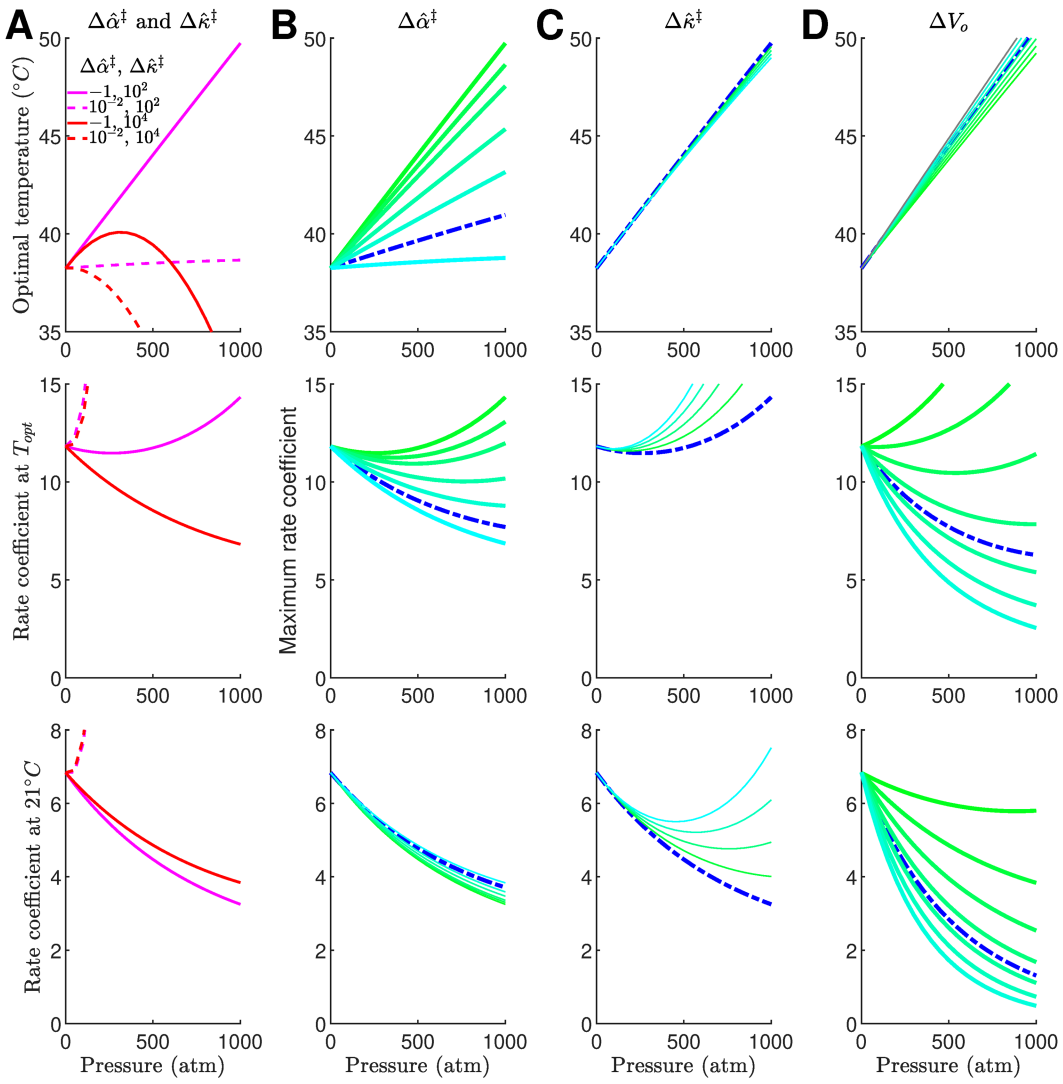

Fig 4. Sensitivity analysis of the rate coefficient function to pressure parameters. (**A**) The optimal temperature (T_{opt}), and rate coefficient at T_{opt}, and at 21 °C when using the combination of the extreme values of $\Delta\hat{\alpha}^{\ddagger}$ and $\Delta\hat{\kappa}^{\ddagger}$.(**B-D**) Sensitivity of the model to individual variations of pressure parameters. The reference model is plotted with a dash blue line in each panel. The range of values were: $\Delta\hat{\alpha}^{\ddagger}$ from –1 to 0 in 0.1 $cm^3mol^{-1}K^{-1}$ increments; $\Delta\hat{\kappa}^{\ddagger}$ from 100 to 500 in 100 $cm^3mol^{-1}GPa^{-1}$ increments; and $\Delta V_o^{\ddagger}$ from 5 to 70 in 10 cm^3mol^{-1} increments. The range of parameters is plotted from low to high value as green to cyan. We used as a reference the model with: P_o = 1atm, T_o = 25°C, $\Delta C_p^{\ddagger}$ = –2.76kJmol^{-1}, $\Delta S_o^{\ddagger}$ – 113Jmol^{-1}K^{-1}, $\Delta H_o^{\ddagger}$ = 34kJmol^{-1}, $\Delta V_o^{\ddagger}$ = 40.96cm^{3}mol^{-1}, $\Delta\hat{\alpha}^{\ddagger}$ = –0.20cm^{3}mol^{-1}K^{-1} and $\Delta\hat{\kappa}^{\ddagger}$ = 10^2cm^{3}mol^{-1}GPa^{-1}.

https://doi.org/10.1371/journal.pone.0333592.g004

simulations in which the Hodgkin-Huxley model was stimulated with random current plus a constant component. We selected the random amplitude and DC offset to generate variable spike trains, Fig 6A. We then used the same random sequence to stimulate an identical model while varying only the pressure. We decided to study lower pressures, including one in the range of intracranial values, 0.02 atm, [35]. These simulations showed that even at very low pressures, the spiking activity could be different from the control simulation, see 1.02 vs 1.00 atm in Fig 6A. As the pressure increased, the spike trains became more different. However, the average firing rate of the entire simulation, 15*sec*, remained basically the

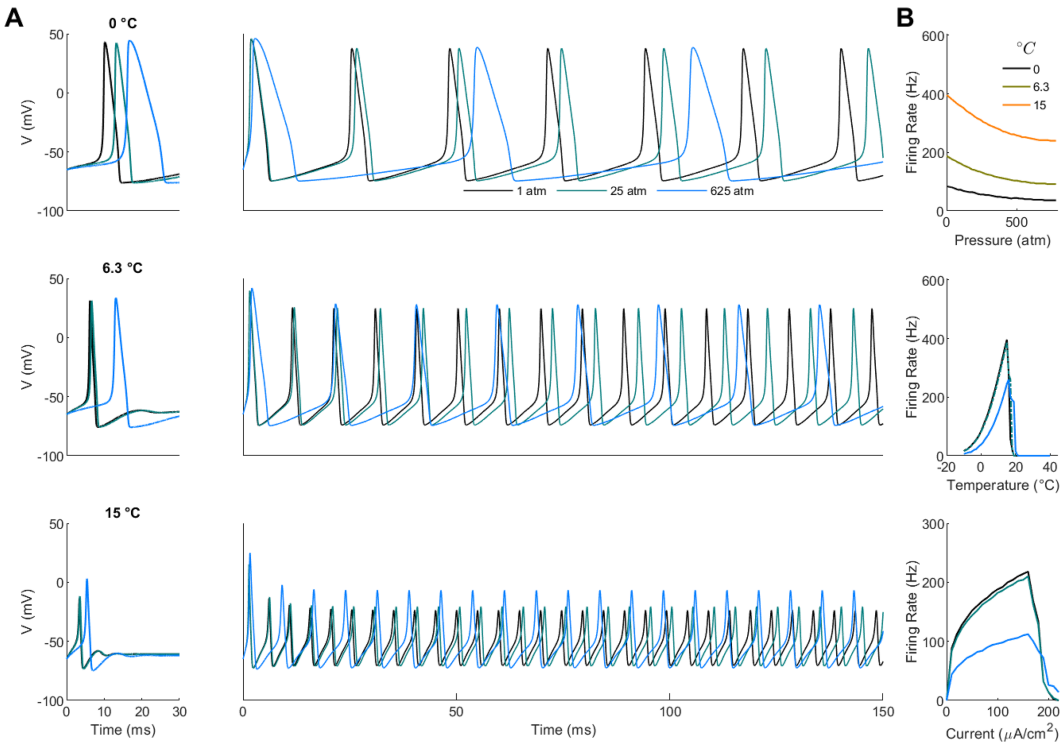

Fig 5. Effects of temperature and pressure on the Hodgkin-Huxley model. (**A**) left - single action potentials generated rheobase for different pressures and temperatures. Right - Spike trains under the same conditions. (**B**) Firing rate vs pressure, temperature, and input current. For each panel the pressure and temperature panels the input current was $100\mu A/cm^2$. For the bottom panel the temperature was 6.3°C.

https://doi.org/10.1371/journal.pone.0333592.g005

same, Fig 6B. To evaluate changes in spiking activity, we calculated the difference in spike time from the control simulation. This pairwise calculation could be constant, corresponding to a shift in the spiking activity. However, the difference in spike time showed variability that seemed to correlate with pressure, Fig 6C. Indeed, when we calculated the standard deviation of the spike differences, there was a pressure effect. These results could be because the simulation at the higher pressure could be slowing down with respect to the control simulation with a dependence on the random noise. However, these differences remained even after averaging multiple simulations (10) using different random number sequences, Fig 6D. In order to test further the idea that the spike trains became decorrelated, we calculated the correlation coefficient of the instantaneous inter-spike interval sequences. This shows that even at the lowest pressure, the spike trains had a low and non-statistically significant correlation coefficient. We binned the ISI sequences in chunks of 10 to test if this correlation could become significant by averaging the noise. Even with this filter, there was only a significant correlation at 1.02 and 2.00 atm, Fig 6E. Together, our results suggest that small pressure changes can affect precise spike timing and correlation of spike trains across neurons.

Finally, we applied the extended theory to biophysical models of human cortical pyramidal cells, see Methods. We analyzed changes in spiking over pressure ranges in blast conditions (10 atm), Fig 7. At these relatively low values of pressure changes the effects were notable in

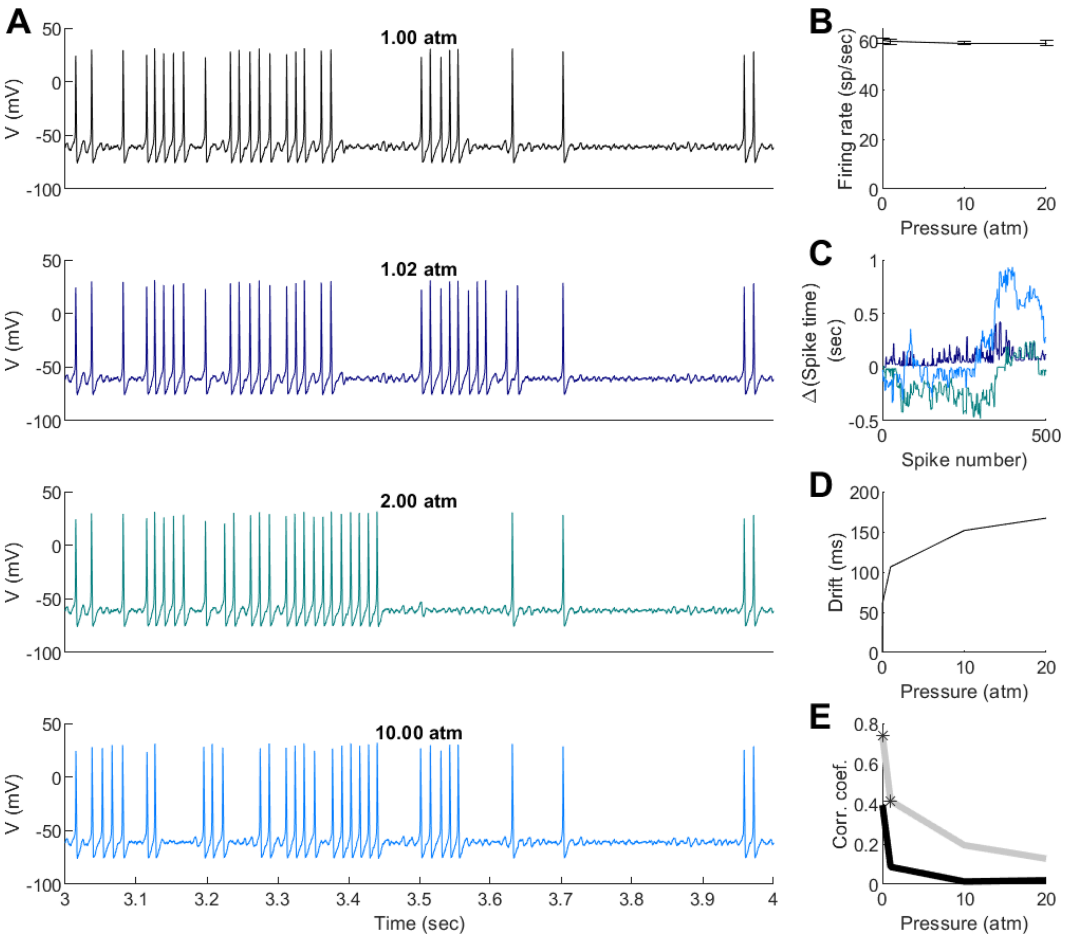

Fig 6. Effects of low-pressure on precise spike timing in the Hodgkin-Huxley model. (**A**) Examples of spike traces of the Hodgkin-Huxley model at different pressure receiving identical sequences of input random currents. For each value of pressure we repeated the simulations 10 times with different input current random sequences. (**B**) Average firing rate vs pressure. Error bars are for the standard deviation calculated on the 10 different runs. (**C**) Examples of spike time differences for simulations that had the same random input sequences of stimulation but different pressures (colors correspond to pressures in A). (**D**) Standard deviation of the spike time differences vs pressure. (**E**) Average correlation coefficients of the inter-spike intervals (ISI) with respect to the simulation at 1 atm (black). We recalculated the correlation coefficients after averaging 10 ISIs, showing two pressures in which the correlations were statistically significant.

https://doi.org/10.1371/journal.pone.0333592.g006

pace-making type neurons. In these and the Hodgkin-Huxley simulation we assumed steady-state temperature and pressure, and so additional temperature change from adiabatic heating was not considered. Overall, our results show that while temperature generally increases the firing rate up to T_{opt}, or up to the point of over-saturation, pressure inhibits or delays action potential generation. While these effects could be mild at the single-cell level, both burst desynchronization between multiple neurons and error in very precise temporal codes could arise from pressure effects.

Discussion

In this work, we combined concepts from MMRT and transition state theory to integrate the effects of temperature, volume, and pressure on the activation energy of voltage-gated

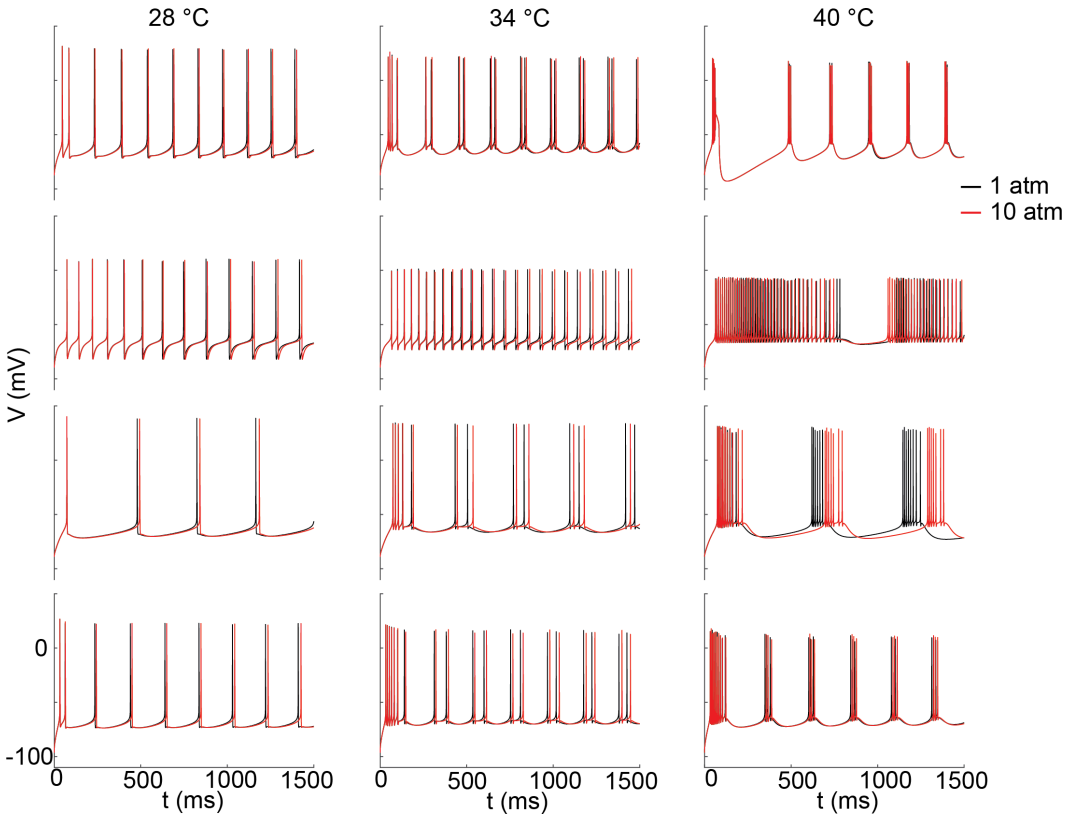

Fig 7. Effects of hypothermic and hyperthermic temperatures and high pressure on the spike trains of models of human cortical pyramidal cells. Rows: four different cortical models. Columns: Three different temperatures. Each model was run with normal and blast-type pressure (10 atm). The models were obtained from the Cell Types database from the Allen Institute, see text for details.

https://doi.org/10.1371/journal.pone.0333592.g007

membrane conductances. While the values of $\Delta H^{\ddagger}$, $\Delta G^{\ddagger}$, and $\Delta S^{\ddagger}$ are well understood, the extended theory uses other variables and parameters that require further understanding.

The activation volume of voltage-gated ion channels

The length of a voltage-gated ion channel (VGIC) is around 45 Å [56–58]. The VGICs are roughly cylindrical [56,58,59] with diameters around 10 Å [56,58,60]. During opening or closing the volume of a pore may change [61–64]. The physical process of activating a channel requires dewetting that can happen by a 1-2 Å decrease in pore radius [61–63]. This simple cylindrical model is an approximation, where real channels often undergo multiple complex conformational changes which all may contribute to $\Delta V^{\ddagger}$. Nevertheless, to gain intuition on the physical meaning of $\Delta V^{\ddagger}$ we will assume a VGIC of height 50 Å and diameter 10 Å. We will also assume that the channel is described by a two-state process, open and closed, Fig 8. Assuming a 1 Å radial decrease when changing states, we can calculate a physical volume difference of $\Delta V^{\ddagger} - V = 2,984 \text{Å}^3 \approx 48 \text{cm}^3/\text{mol}$ which is on the same scale as values found in multiple experiments [29–32,45–47]. This similarity between geometrically and experimentally determined values of activation volume lead us to propose that these properties could be physically modeled based on protein structure, instead of fitting and estimating them, and could be an interesting future direction of research.

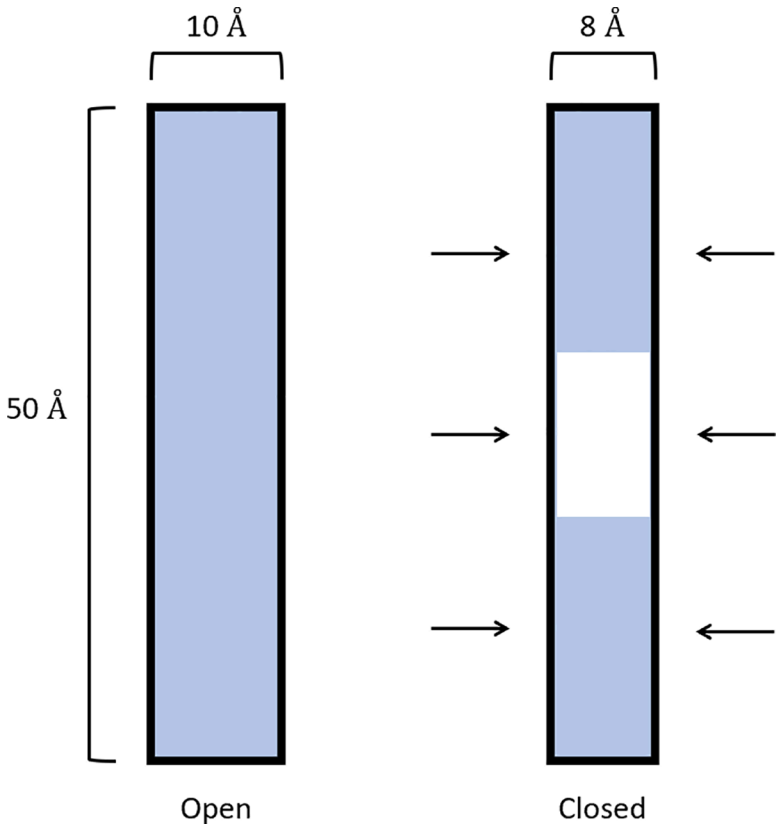

Fig 8. Simplified pore cross section during open and closed states. In the closed state, the radius shrinks by 1 Å which allows the fully hydrophobic part of the pore to dewet. The blue represents regions occupied by water molecules.

https://doi.org/10.1371/journal.pone.0333592.g008

Expansivity, compressibility, and further development

Just as $\Delta V^{\ddagger}$ allows suggestions of underlying mechanisms such as pore constriction, expansivity and compressibility may offer insights into the greater complexity behind pressure and volume effects on ion channels. For instance, compressibility is relevant to aromatic ring flip conformations of proteins [39]. Positive transition compressibility suggests that the ion channel volume is more susceptible to pressure when open. Expansivity is an important parameter as it sets the temperature dependence of activation volume. If transition expansivity is positive, one would suspect channel volume to be less partial to temperature when closed. Intuitively, this seems to contradict the concept of a closed, evacuated pore as liquid water in the open state should be less expansive. That interpretation makes negative transition values seem more plausible.

Conceptually, $\Delta\hat{\alpha}^{\ddagger}$ is the difference in the partial temperature derivative of volume between the transition and ground states of a reaction. The derivatives can be large, but if we take the high value of the parameter $\Delta\hat{\alpha}^{\ddagger} = -1$ and Eq 13b with our reported $\Delta V_o^{\ddagger}$ we can see that just a 19°C increase would set $\Delta V^{\ddagger} = 0$. Negative activation volumes are possible for processes such as unfolding [43], but are likely nonphysical for gate opening. That value also implies an extreme 100% change in activation volume. The same applies for a high compressibility of $\Delta\hat{\kappa}^{\ddagger} = 10,000$ which suggests activation volume would be zero after about 20atm

of pressure which we know cannot be true from the experimental data. So, the T_{opt} is not a significant function of pressure.

Finally, it should be noted that $\Delta C_p^{\ddagger}$, $\Delta\hat{\alpha}^{\ddagger}$, and $\Delta\hat{\kappa}^{\ddagger}$ may all depend on the pressure and temperature themselves. We mentioned that $\Delta C_p^{\ddagger}$ is assumed constant, but it could be given a linear temperature dependence [17], some parameter-based function of temperature and pressure [65], and it has been suggested to increase with pressure [66]. If $\Delta C_p^{\ddagger}$ had a significant pressure dependence, it could also explain the apparent temperature dependence of $\Delta V^{\ddagger}$, rather than or in addition to $\Delta\hat{\alpha}^{\ddagger}$. For simplicity, we did not include adiabatic heating in our simulations. Any of these effects, if significant at a biological temperature range or at high pressures, would limit the model at its current level of detail, but not necessarily invalidate the modeling strategy. Though, outside of biological ranges, where there is protein denaturation or cell death, the model regardless of parameters would certainly no longer apply.

Conclusion

We presented thermodynamic theory that can be integrated with studies of neuronal excitability [67,68]. More broadly, a unified temperature and pressure theory can be used to compare the enzymatic kinetics of diving creatures and extremophilic bacteria in hundreds of atmospheres in the ocean [20,21,34] with land creatures or their ancestors. Our work provides a platform to study the evolution of preferred body temperatures [33] with the optimal temperature of enzymes. Pressure has mechanical consequences for neuronal function and structure [69,70] due to membrane mechanics. In the context of human health, changes in intracranial pressure (ICP) can arise from many phenomena such as intracerebral hemorrhage [71], plateau waves [72], microgravity [73], and impacts and blasts [35,36]. For example, acceleration effects can change the ICP and have been shown to have negative effects on cognitive performance [74,75]. Pressure changes caused by ICP are around 10-100 mmHg (0.05atm) which we showed have little effect on the firing rate [76], but that could affect precise spike timing. It remains to evaluate in a similar way if the small pressure changes from action potential propagation [9] could have a significant effect. In any case, our work suggests that pressure affects precise spike timing and we suggest that cumulative effects could modify network dynamics and performance. The mechanisms we describe could combine with other cellular communication mechanisms important for network activity, such as the effects of pressure on synaptic release [47]. Other areas to consider are how membrane thermodynamics affect anesthesia [37,38] and how membrane changes could alter channel function [7]. While in this study we focused on developing theory for applications on neuronal intrinsic excitability driven by voltage activated ion channels there could be other emergent network-level effects or intracellular metabolic pathways that together could enrich the thermodynamical effects on neuronal and network function. As such, our work promotes the return to experimentation and discussion of pressure, especially since pressure experiments can reveal important biological properties [77].

Author contributions

Conceptualization: Jake A. Miller, Fidel Santamaria.

Formal analysis: Jake A. Miller, Bahram Pahlavan.

Funding acquisition: Bryan Gamboa, Fidel Santamaria.

Investigation: Jake A. Miller, Fidel Santamaria.

Methodology: Jake A. Miller, Fidel Santamaria.

Project administration: Fidel Santamaria.

Software: Jake A. Miller, Fidel Santamaria.

Supervision: Bryan Gamboa, Fidel Santamaria.

Validation: Fidel Santamaria.

Visualization: Jake A. Miller, Bahram Pahlavan.

Writing – original draft: Jake A. Miller, Bahram Pahlavan, Fidel Santamaria.

Writing – review & editing: Jake A. Miller, Bryan Gamboa, Fidel Santamaria.

References

1. Hodgkin AL, Katz B. The effect of temperature on the electrical activity of the giant axon of the squid. J Physiol. 1949;109(1–2):240–9. https://doi.org/10.1113/jphysiol.1949.sp004388 PMID: 15394322
2. Burek M, Follmann R, Rosa E. Temperature effects on neuronal firing rates and tonic-to-bursting transitions. Biosystems. 2019;180:1–6. https://doi.org/10.1016/j.biosystems.2019.03.003 PMID: 30862447
3. Miller JD, Cao VH, Heller HC. Thermal effects on neuronal activity in suprachiasmatic nuclei of hibernators and nonhibernators. Am J Physiol. 1994;266(4 Pt 2):R1259-66. https://doi.org/10.1152/ajpregu.1994.266.4.R1259 PMID: 8184970
4. Jabbari MB, Karamati MR. The effects of temperature on the dynamics of the biological neural network. J Biol Phys. 2022;48(1):111–26. https://doi.org/10.1007/s10867-021-09598-1 PMID: 35064447
5. Almog M, Degani-Katzav N, Korngreen A. Kinetic and thermodynamic modeling of a voltage-gated sodium channel. Eur Biophys J. 2022;51(3):241–56. https://doi.org/10.1007/s00249-022-01591-3 PMID: 35199191
6. Tkachenko Y, Khmyz V, Isaev D, Maximyuk O, Krishtal O. Temperature increase significantly enhances nociceptive responses of C-fibers to ATP, high K+, and acidic pH in mice. Front Cell Neurosci. 2023;17:1131643. https://doi.org/10.3389/fncel.2023.1131643 PMID: 36846206
7. Lundbaek JA, Birn P, Girshman J, Hansen AJ, Andersen OS. Membrane stiffness and channel function. Biochemistry. 1996;35(12):3825–30. https://doi.org/10.1021/bi952250b PMID: 8620005
8. Martinac B, Buechner M, Delcour AH, Adler J, Kung C. Pressure-sensitive ion channel in Escherichia coli. Proc Natl Acad Sci U S A. 1987;84(8):2297–301. https://doi.org/10.1073/pnas.84.8.2297 PMID: 2436228
9. Terakawa S. Potential-dependent variations of the intracellular pressure in the intracellularly perfused squid giant axon. J Physiol. 1985;369:229–48. https://doi.org/10.1113/jphysiol.1985.sp015898 PMID: 4093881
10. Arrhenius S. Über die Dissociationswärme und den Einfluss der Temperatur auf den Dissociationsgrad der Elektrolyte. Zeitschrift für Physikalische Chemie. 1889;4U(1):96–116. https://doi.org/10.1515/zpch-1889-0408
11. Truhlar DG, Garrett BC, Klippenstein SJ. Current status of transition-state theory. J Phys Chem. 1996;100(31):12771–800. https://doi.org/10.1021/jp953748q
12. Elias M, Wieczorek G, Rosenne S, Tawfik DS. The universality of enzymatic rate-temperature dependency. Trends Biochem Sci. 2014;39(1):1–7. https://doi.org/10.1016/j.tibs.2013.11.001 PMID: 24315123
13. Pahlavan B, Buitrago N, Santamaria F. Macromolecular rate theory explains the temperature dependence of membrane conductance kinetics. Biophys J. 2023;122(3):522–32. https://doi.org/10.1016/j.bpj.2022.12.033 PMID: 36567527
14. Wei G, Xi W, Nussinov R, Ma B. Protein ensembles: how does nature harness thermodynamic fluctuations for life? The diverse functional roles of conformational ensembles in the cell. Chem Rev. 2016;116(11):6516–51. https://doi.org/10.1021/acs.chemrev.5b00562 PMID: 26807783
15. Winter R, Dzwolak W. Exploring the temperature-pressure configurational landscape of biomolecules: from lipid membranes to proteins. Philos Trans A Math Phys Eng Sci. 2005;363(1827):537–62; discussion 562-3. https://doi.org/10.1098/rsta.2004.1507 PMID: 15664898

16. Hobbs JK, Jiao W, Easter AD, Parker EJ, Schipper LA, Arcus VL. Change in heat capacity for enzyme catalysis determines temperature dependence of enzyme catalyzed rates. ACS Chem Biol. 2013;8(11):2388–93. https://doi.org/10.1021/cb4005029 PMID: 24015933

17. Prabhu NV, Sharp KA. Heat capacity in proteins. Annu Rev Phys Chem. 2005;56:521–48. https://doi.org/10.1146/annurev.physchem.56.092503.141202 PMID: 15796710

18. Wann KT, Macdonald AG. The effects of pressure on excitable cells. Comparative Biochemistry and Physiology Part A: Physiology. 1980;66(1):1–12. https://doi.org/10.1016/0300-9629(80)90353-9

19. Morild E. The theory of pressure effects on enzymes. Adv Protein Chem. 1981;34:93–166. https://doi.org/10.1016/s0065-3233(08)60519-7 PMID: 7020377

20. Heremans K. High pressure effects on proteins and other biomolecules. Annu Rev Biophys Bioeng. 1982;11:1–21. https://doi.org/10.1146/annurev.bb.11.060182.000245 PMID: 7049058

21. Heremans K, Smeller L. Protein structure and dynamics at high pressure. Biochim Biophys Acta. 1998;1386(2):353–70. https://doi.org/10.1016/s0167-4838(98)00102-2 PMID: 9733996

22. Balny C, Masson P, Heremans K. High pressure effects on biological macromolecules: from structural changes to alteration of cellular processes. Biochim Biophys Acta. 2002;1595(1–2):3–10. https://doi.org/10.1016/s0167-4838(01)00331-4 PMID: 11983383

23. Ross-Rodriguez LU, Elliott JAW, McGann LE. Non-ideal solution thermodynamics of cytoplasm. Biopreserv Biobank. 2012;10(5):462–71. https://doi.org/10.1089/bio.2012.0027 PMID: 23840923

24. Elliott JAW, Prickett RC, Elmoazzen HY, Porter KR, McGann LE. A multisolute osmotic virial equation for solutions of interest in biology. J Phys Chem B. 2007;111(7):1775–85. https://doi.org/10.1021/jp0680342 PMID: 17266364

25. Acerbo P, Nobile M. Temperature dependence of multiple high voltage activated Ca2+ channels in chick sensory neurones. Eur Biophys J. 1994;23(3):189–95. https://doi.org/10.1007/BF01007610 PMID: 7525267

26. Cao X-J, Oertel D. Temperature affects voltage-sensitive conductances differentially in octopus cells of the mammalian cochlear nucleus. J Neurophysiol. 2005;94(1):821–32. https://doi.org/10.1152/jn.01049.2004 PMID: 15800074

27. Egri C, Vilin YY, Ruben PC. A thermoprotective role of the sodium channel β1 subunit is lost with the β1 (C121W) mutation. Epilepsia. 2012;53(3):494–505. https://doi.org/10.1111/j.1528-1167.2011.03389.x PMID: 22292491

28. Bassetto CA, Pinto BI, Latorre R, Bezanilla F. ION channel thermodynamics studied with temperature jumps measured at the membrane. bioRxiv. 2022. 2022–07.

29. Conti F, Fioravanti R, Segal JR, Stühmer W. The effect of hydrostatic pressure on the voltage-clamp currents of the squid giant axon. Developments in biophysical research. Springer US. 1980. p. 25–33. https://doi.org/10.1007/978-1-4684-1077-8_3

30. Conti F, Fioravanti R, Segal JR, Stühmer W. Pressure dependence of the potassium currents of squid giant axon. J Membr Biol. 1982;69(1):35–40. https://doi.org/10.1007/BF01871239 PMID: 7120362

31. Conti F, Fioravanti R, Segal JR, Stühmer W. Pressure dependence of the sodium currents of squid giant axon. J Membr Biol. 1982;69(1):23–34. https://doi.org/10.1007/BF01871238 PMID: 7120361

32. Conti F, Inoue I, Kukita F, Stühmer W. Pressure dependence of sodium gating currents in the squid giant axon. Eur Biophys J. 1984;11(2):137–47. https://doi.org/10.1007/BF00276629 PMID: 6100544

33. Arcus VL, van der Kamp MW, Pudney CR, Mulholland AJ. Enzyme evolution and the temperature dependence of enzyme catalysis. Curr Opin Struct Biol. 2020;65:96–101. https://doi.org/10.1016/j.sbi.2020.06.001 PMID: 32659635

34. Macdonald AG. Ion channels under high pressure. Comp Biochem Physiol A Mol Integr Physiol. 2002;131(3):587–93. https://doi.org/10.1016/s1095-6433(01)00510-4 PMID: 11867284

35. Chafi MS, Karami G, Ziejewski M. Biomechanical assessment of brain dynamic responses due to blast pressure waves. Ann Biomed Eng. 2010;38(2):490–504. https://doi.org/10.1007/s10439-009-9813-z PMID: 19806456

36. Hosseini-Farid M, Amiri-Tehrani-Zadeh M, Ramzanpour M, Ziejewski M, Karami G. The strain rates in the brain, brainstem, dura, and skull under dynamic loadings. MCA. 2020;25(2):21. https://doi.org/10.3390/mca25020021

37. Jerusalem A, Al-Rekabi Z, Chen H, Ercole A, Malboubi M, Tamayo-Elizalde M, et al. Electrophysiological-mechanical coupling in the neuronal membrane and its role in ultrasound neuromodulation and general anaesthesia. Acta Biomater. 2019;97:116–40. https://doi.org/10.1016/j.actbio.2019.07.041 PMID: 31357005

38. Heimburg T. The thermodynamic soliton theory of the nervous impulse and possible medical implications. Prog Biophys Mol Biol. 2022;173:24–35. https://doi.org/10.1016/j.pbiomolbio.2022.05.007 PMID: 35640761

39. Dreydoppel M, Dorn B, Modig K, Akke M, Weininger U. Transition-state compressibility and activation volume of transient protein conformational fluctuations. JACS Au. 2021;1(6):833–42. https://doi.org/10.1021/jacsau.1c00062 PMID: 34467336

40. Schipper LA, Hobbs JK, Rutledge S, Arcus VL. Thermodynamic theory explains the temperature optima of soil microbial processes and high Q10 values at low temperatures. Glob Chang Biol. 2014;20(11):3578–86. https://doi.org/10.1111/gcb.12596 PMID: 24706438

41. Asano T, Le Noble WJ. Activation and reaction volumes in solution. Chem Rev. 1978;78(4):407–89. https://doi.org/10.1021/cr60314a004

42. Low PS, Somero GN. Activation volumes in enzymic catalysis: their sources and modification by low-molecular-weight solutes. Proc Natl Acad Sci U S A. 1975;72(8):3014–8. https://doi.org/10.1073/pnas.72.8.3014 PMID: 1059089

43. Royer CA. Revisiting volume changes in pressure-induced protein unfolding. Biochim Biophys Acta. 2002;1595(1–2):201–9. https://doi.org/10.1016/s0167-4838(01)00344-2 PMID: 11983396

44. Le Noble W. Kinetics of reactions in solutions under pressure. Prog Phys Org Chem. 1967;5:207–330.

45. Henderson JV Jr, Gilbert DL. Slowing of ionic currents in the voltage-clamped squid axon by helium pressure. Nature. 1975;258(5533):351–2. https://doi.org/10.1038/258351a0 PMID: 1196366

46. Heinemann SH, Stühmer W, Conti F. Single acetylcholine receptor channel currents recorded at high hydrostatic pressures. Proc Natl Acad Sci U S A. 1987;84(10):3229–33. https://doi.org/10.1073/pnas.84.10.3229 PMID: 2437577

47. Heinemann SH, Conti F, Stühmer W, Neher E. Effects of hydrostatic pressure on membrane processes. Sodium channels, calcium channels, and exocytosis. J Gen Physiol. 1987;90(6):765–78. https://doi.org/10.1085/jgp.90.6.765 PMID: 2450167

48. Meyer R, Heinemann SH. Temperature and pressure dependence of Shaker K+ channel N- and C-type inactivation. Eur Biophys J. 1997;26(6):433–45. https://doi.org/10.1007/s002490050098 PMID: 9404006

49. Shushakov VV, Demchenko IT. Dynamics of ion currents in the membrane of the isolated mollusc neuron under high pressure. Neurosci Behav Physiol. 1996;26(3):241–4. https://doi.org/10.1007/BF02360688 PMID: 8823740

50. Seemann H, Winter R, Royer CA. Volume, expansivity and isothermal compressibility changes associated with temperature and pressure unfolding of Staphylococcal nuclease. J Mol Biol. 2001;307(4):1091–102. https://doi.org/10.1006/jmbi.2001.4517 PMID: 11286558

51. Lin L-N, Brandts JF, Brandts JM, Plotnikov V. Determination of the volumetric properties of proteins and other solutes using pressure perturbation calorimetry. Anal Biochem. 2002;302(1):144–60. https://doi.org/10.1006/abio.2001.5524 PMID: 11846388

52. Gekko Kunihiko, Noguchi Hajime. Compressibility of globular proteins in water at 25.degree.C. J Phys Chem. 1979;83(21):2706–14. https://doi.org/10.1021/j100484a006

53. Royer C, Winter R. Protein hydration and volumetric properties. Current Opinion in Colloid & Interface Science. 2011;16(6):568–71. https://doi.org/10.1016/j.cocis.2011.04.008

54. Persson F, Halle B. Compressibility of the protein-water interface. J Chem Phys. 2018;148(21):215102. https://doi.org/10.1063/1.5026774 PMID: 29884062

55. Spyropoulos CS. Response of single nerve fibers at different hydrostatic pressures. Am J Physiol. 1957;189(1):214–8. https://doi.org/10.1152/ajplegacy.1957.189.1.214 PMID: 13424720

56. Doyle DA, Morais Cabral J, Pfuetzner RA, Kuo A, Gulbis JM, Cohen SL, et al. The structure of the potassium channel: molecular basis of K+ conduction and selectivity. Science. 1998;280(5360):69–77. https://doi.org/10.1126/science.280.5360.69 PMID: 9525859

57. Shaya D, Findeisen F, Abderemane-Ali F, Arrigoni C, Wong S, Nurva SR, et al. Structure of a prokaryotic sodium channel pore reveals essential gating elements and an outer ion binding site common to eukaryotic channels. J Mol Biol. 2014;426(2):467–83. https://doi.org/10.1016/j.jmb.2013.10.010 PMID: 24120938

58. Hering S, Zangerl-Plessl E-M, Beyl S, Hohaus A, Andranovits S, Timin EN. Calcium channel gating. Pflugers Arch. 2018;470(9):1291–309. https://doi.org/10.1007/s00424-018-2163-7 PMID: 29951751

59. Sula A, Booker J, Ng LCT, Naylor CE, DeCaen PG, Wallace BA. The complete structure of an activated open sodium channel. Nat Commun. 2017;8:14205. https://doi.org/10.1038/ncomms14205 PMID: 28205548

60. Lenaeus MJ, Gamal El-Din TM, Ing C, Ramanadane K, Pomès R, Zheng N, et al. Structures of closed and open states of a voltage-gated sodium channel. Proc Natl Acad Sci U S A. 2017;114(15):E3051–60. https://doi.org/10.1073/pnas.1700761114 PMID: 28348242

61. Zhang XC, Yang H, Liu Z, Sun F. Thermodynamics of voltage-gated ion channels. Biophys Rep. 2018;4(6):300–19. https://doi.org/10.1007/s41048-018-0074-y PMID: 30596139

62. Yazdani M, Jia Z, Chen J. Hydrophobic dewetting in gating and regulation of transmembrane protein ion channels. J Chem Phys. 2020;153(11):110901. https://doi.org/10.1063/5.0017537 PMID: 32962356

63. Aryal P, Sansom MSP, Tucker SJ. Hydrophobic gating in ion channels. J Mol Biol. 2015;427(1):121–30. https://doi.org/10.1016/j.jmb.2014.07.030 PMID: 25106689

64. Jensen MØ, Borhani DW, Lindorff-Larsen K, Maragakis P, Jogini V, Eastwood MP, et al. Principles of conduction and hydrophobic gating in K+ channels. Proc Natl Acad Sci U S A. 2010;107(13):5833–8. https://doi.org/10.1073/pnas.0911691107 PMID: 20231479

65. Jovanović JD, Knežević-Stevanović AB, Grozdanić DK. An empirical equation for temperature and pressure dependence of liquid heat capacity. Journal of the Taiwan Institute of Chemical Engineers. 2009;40(1):105–9.

66. Drebushchak VA. Heat capacity increases with pressure. J Therm Anal Calorim. 2008;95(1):313–7. https://doi.org/10.1007/s10973-008-9221-x

67. Ben-Abu Y, Tucker SJ, Contera S. Transcending Markov: non-Markovian rate processes of thermosensitive TRP ion channels. R Soc Open Sci. 2023;10(8):230984. https://doi.org/10.1098/rsos.230984 PMID: 37621668

68. Kim T, Kadji H, Whalen AJ, Ashourvan A, Freeman E, Fried SI, et al. Thermal effects on neurons during stimulation of the brain. J Neural Eng. 2022;19(5):056029. https://doi.org/10.1088/1741-2552/ac9339 PMID: 36126646

69. Jiang H, Sun SX. Cellular pressure and volume regulation and implications for cell mechanics. Biophys J. 2013;105(3):609–19. https://doi.org/10.1016/j.bpj.2013.06.021 PMID: 23931309

70. Mueller JK, Tyler WJ. A quantitative overview of biophysical forces impinging on neural function. Phys Biol. 2014;11(5):051001. https://doi.org/10.1088/1478-3975/11/5/051001 PMID: 25156965

71. Guo T, Ren P, Li X, Luo T, Gong Y, Hao S, et al. Neural injuries induced by hydrostatic pressure associated with mass effect after intracerebral hemorrhage. Sci Rep. 2018;8(1):9195. https://doi.org/10.1038/s41598-018-27275-7 PMID: 29907795

72. Dias C, Maia I, Cerejo A, Varsos G, Smielewski P, Paiva J-A, et al. Pressures, flow, and brain oxygenation during plateau waves of intracranial pressure. Neurocrit Care. 2014;21(1):124–32. https://doi.org/10.1007/s12028-013-9918-y PMID: 24072460

73. Lawley JS, Petersen LG, Howden EJ, Sarma S, Cornwell WK, Zhang R, et al. Effect of gravity and microgravity on intracranial pressure. J Physiol. 2017;595(6):2115–27. https://doi.org/10.1113/JP273557 PMID: 28092926

74. Ercan E, Gunduz SH. The effects of acceleration forces on cognitive functions. Microgravity Sci Technol. 2020;32(4):681–6. https://doi.org/10.1007/s12217-020-09793-0

75. McKinlly RA, Gallimore JJ. Computational model of sustained acceleration effects on human cognitive performance. Aviat Space Environ Med. 2013;84(8):780–8. https://doi.org/10.3357/asem.2584.2013 PMID: 23926652

76. Mizunuma M, Takahashi N, Usami A, Matsuki N, Ikegaya Y. High-temperature, but not high-pressure, conditions alter neuronal activity. J Pharmacol Sci. 2009;110(1):117–21. https://doi.org/10.1254/jphs.09031sc PMID: 19430196

77. Meersman F, McMillan PF. High hydrostatic pressure: a probing tool and a necessary parameter in biophysical chemistry. Chem Commun (Camb). 2014;50(7):766–75. https://doi.org/10.1039/c3cc45844j PMID: 24286104